Amino Acids
https://doi.org/10.1007/s00726-018-2656-x

ORIGINAL ARTICLE

Studies on acid stability and solid-phase block synthesis of peptide–peptoid hybrids: ligands for formyl peptide receptors

Anna Mette Hansen[1] · **Sarah Line Skovbakke**[2] · **Simon Bendt Christensen**[1] · **Iris Perez-Gassol**[1] · **Henrik Franzyk**[1]

Received: 4 July 2018 / Accepted: 17 September 2018

Abstract

α-Peptoids as well as peptide/α-peptoid hybrids and peptide/β-peptoid hybrids constitute major classes of proteolytically stable peptidomimetics that have been extensively investigated as mimetics of biologically active peptides. Representatives of lipidated peptide/β-peptoid hybrids have been identified as promising immunomodulatory lead compounds, and hence access to these via protocols suitable for gram-scale synthesis is warranted to enable animal in vivo studies. Recent observations indicated that several byproducts appear in crude mixtures of relatively short benzyl-based peptide/β-peptoid oligomers, and that these were most predominant when the β-peptoid units displayed an α-chiral benzyl side chain. This prompted an investigation of their stability under acidic conditions. Simultaneous deprotection and cleavage of peptidomimetics containing either α-chiral α- or β-peptoid residues required treatment with strong acid only for a short time to minimize the formation of partially debenzylated byproducts. The initial work on peptide/β-peptoid oligomers with an alternating design established that it was beneficial to form the amide bond between the carboxyl group of the α-amino acid and the congested amino functionality of the β-peptoid residue in solution. To further simplify oligomer assembly on solid phase, we now present a protocol for purification-free solid-phase synthesis of tetrameric building blocks. Next, syntheses of peptidomimetic ligands via manual solid-phase methodologies involving tetrameric building blocks were found to give more readily purified products as compared to those obtained with dimeric building blocks. Moreover, the tetrameric building blocks could be utilized in automated synthesis with microwave-assisted heating, albeit the purity of the crude products was not increased.

Keywords Peptidomimetics · Peptoids · Solid-phase synthesis · Acid stability · Formyl peptide receptor ligands

Introduction

As a consequence of the inherently low stability of drugs based on natural peptides, several classes of peptidomimetics have been explored to overcome this drawback (Mojsoska and Jenssen 2015; Molchanova et al. 2017). Peptoids constitute a class of proteolytically stable peptidomimetics consisting of N-substituted glycine residues, and thus peptoids differ from α-peptides in having the side chains attached to the backbone nitrogen atoms instead of at the C-α atoms (Fig. 1). Moreover, since peptide–peptoid hybrids or even peptoid homooligomers often can be designed to mimic the biological activity of a parent peptide, while gaining stability toward proteases, these peptidomimetics are considered as potential therapeutics as reviewed elsewhere (Zuckermann and Kodadek 2009; Fowler and Blackwell 2009; Zuckermann 2011; Hansen and Munk 2013).

Handling Editor: F. Albericio.

Electronic supplementary material The online version of this article (https://doi.org/10.1007/s00726-018-2656-x) contains supplementary material, which is available to authorized users.

✉ Henrik Franzyk
henrik.franzyk@sund.ku.dk

[1] Department of Drug Design and Pharmacology, Faculty of Health and Medical Sciences, University of Copenhagen, Jagtvej 162, 2100 Copenhagen, Denmark

[2] Department of Veterinary and Animal Sciences, Faculty of Health and Medical Sciences, University of Copenhagen, Rolighedsvej 25b, 1958 Frederiksberg, Denmark

Published online: 28 September 2018

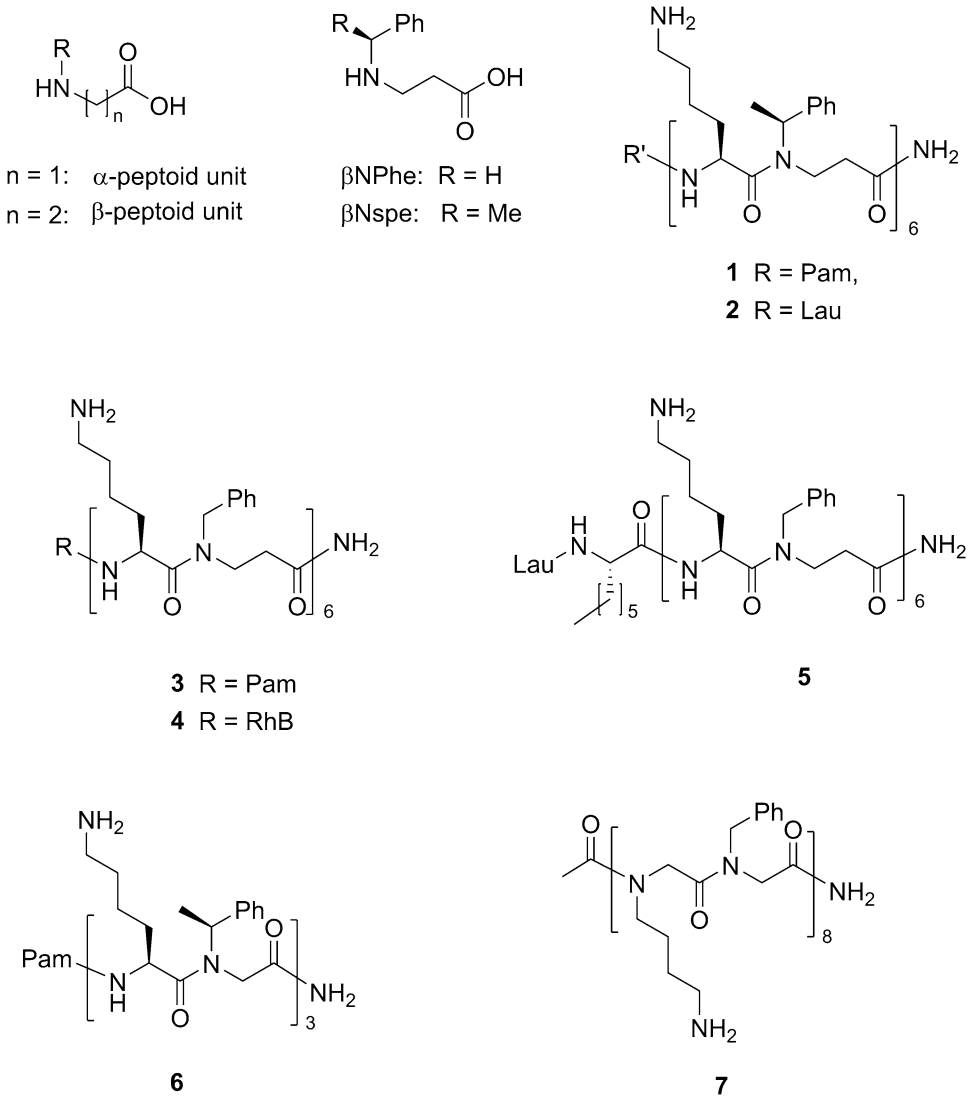

Fig. 1 Target compounds and structure of peptoid units. *Lau* lauroyl, *Pam* palmitoyl

In particular, antimicrobial peptoid homooligomers have been designed and studied by several research groups (Goodson et al. 1999; Chongsiriwatana et al. 2008; Bang et al. 2010; Findlay et al. 2012; Mojsoska et al. 2015; Bolt et al. 2017), while other contributions have focused on the exploration of the effects of introducing peptoid residues as a means of disrupting the α-helical secondary structure of antimicrobial peptides to diminish toxicity induced by a high degree of amphipathicity (Kim et al. 2010; Shin 2014). In addition, antibacterial peptide–peptoid hybrids with a high content of peptoid residues have been investigated (Ryge et al. 2008; Lin et al. 2016). While only two reports on antibacterial β-peptoid homooligomers have appeared so far (Shuey et al. 2006; Jahnsen et al. 2012), the class of α-peptide/β-peptoid hybrids with an alternating design has been extensively investigated as potential antimicrobials (Jahnsen et al. 2012, 2014; Hein-Kristensen et al. 2011; Liu et al. 2013) as well as for their immunomodulatory effects when modified with hydrophobic headgroups, e.g., as seen for compounds **1**–**5** depicted in Fig. 1 (Skovbakke et al. 2015a, b, 2016, 2017; Holdfeldt et al. 2016). Thus, while the α-peptide/α-peptoid hybrid Ac-[Lys-NPhe]$_8$-NH$_2$ only displayed modest anti-inflammatory effects (Jahnsen et al. 2013), the lipidated α-peptide/β-peptoid hybrid Pam-[Lys-βNspe]$_6$-NH$_2$ (**1**) was found to neutralize LPS- and LTA-induced pro-inflammatory responses from human leukocytes with IC$_{50}$ values of 60 nM and 0.85 µM (measured for IL-6 secretion), respectively (Skovbakke et al. 2015b).

Moreover, compounds **1** and **3** were recently identified as selective antagonists of human neutrophilic formyl peptide receptor 2 (FPR2) (Skovbakke et al. 2015a). Thus, FPR2-induced NADPH-oxidase responses and degranulation were inhibited by **1** and **3** with a potency (IC$_{50}$ values of 50 nM and 60 nM, respectively) similar to that of the gelsolin-derived peptide PBP10 displaying an N-terminal rhodamine B (RhB) moiety (Forsman et al. 2012; Skovbakke

et al. 2015a). In addition, the closely related analog Lau-[Lys-βNspe]$_6$-NH_2 (**2**) proved to be a potent antagonist of the mouse orthologue Fpr2, thereby establishing the first class of compounds that exhibit cross-species activity with retained receptor selectivity (Skovbakke et al. 2016), which will enable the exploration of the role of FRP2 in innate immunity via mouse models. Recently, the designed PBP10-peptidomimetic hybrid, RhB-[Lys-βNPhe]$_6$-NH_2 (**4**), was found to possess potent antagonistic activity at FPR2 (with an IC_{50} value of 15 nM) (Skovbakke et al. 2017). This novel class of selective nanomolar FPR2 antagonists constitutes potential lead compounds for the development of novel anti-inflammatory drugs.

Screening of an array of lipidated α-peptide/β-peptoid hybrids, displaying headgroups with two hydrophobic moieties, led to the identification of Lau-[(*S*)-Aoc]-[Lys-βNPhe]$_6$-NH_2 (**5**; Aoc = 2-aminooctanoic acid) as a potent FPR2 agonist that activated both human and mouse neutrophil NADPH-oxidase (EC_{50} values of 167 nM and 82 nM, respectively) (Holdfeldt et al. 2016). The structural prerequisites for high agonistic potency proved to be quite specific, since analogs displaying slightly shorter or longer fatty acid tails (e.g., C_{10} or C_{14} instead of C_{12}) were considerably less efficient, while replacement of (*S*)-Aoc with residues having shorter/longer alkyl side chains lacked agonistic activity, and introduction of (*R*)-Aoc also led to compromised activity (Holdfeldt et al. 2016). This subclass of lipidated α-peptide/β-peptoid hybrids appears to constitute a valuable tool in mechanistic studies of FPR2 signaling in vivo as well as a source of potential leads for prophylactic anti-infectives stimulating bacterial clearance by neutrophils.

In view of the interesting biological activities exerted by the different subclasses of peptide/peptoid hybrids (Olsen 2010; Molchanova et al. 2017) we considered how to device an efficient protocol suitable for gram-scale synthesis. The initial work concerning solid-phase synthesis of β-peptoid oligomers, consisting of α-chiral βNspe residues, had shown that both submonomer and monomer approaches were challenging. In the submonomer methodology, involving on-resin aza-Michael addition of a sterically hindered α-chiral primary amine [e.g., (*S*)-1-phenylethylamine] to a resin-bound acrylic amide, complete conversion in each elongation step proved difficult to achieve within a reasonably short reaction time (Norgren et al. 2006; Olsen et al. 2008). Likewise, sequential assembly of preformed Fmoc-βNspe-OH monomers, displaying a congested secondary amine, was problematic even when using TFFH for in situ formation of acyl fluorides as a means for overcoming sterical hindrance in the amide couplings (Olsen et al. 2008). As an alternative versatile strategy, multigram-scale protocols for solution-phase synthesis of dimeric building blocks were developed for both α-peptide/α-peptoid and α-peptide/β-peptoid oligomers (Jahnsen et al. 2014; Bonke et al. 2008). Thus, nucleophilic substitution of *tert*-butyl α-bromoacetate with an appropriate primary amine gave a C-terminally protected α-peptoid intermediate (Jahnsen et al. 2012, 2014; Simon et al. 1992; Zuckermann et al. 1992; Kruijtzer et al. 1998), while aza-Michael addition of the appropriate primary amine to *tert*-butyl acrylate afforded the corresponding β-peptoid intermediate (Bonke et al. 2008). In both cases, the peptoid intermediates were subjected to solution-phase coupling with a commercial Fmoc-protected lysine building block to give the fully protected intermediates that were converted into the final dimeric building blocks in one-pot procedures (Jahnsen et al. 2014; Bonke et al. 2008). Assembly of such dimeric building blocks into longer oligomers (typically 10–16 residues) can readily be performed via solid-phase protocols (Jahnsen et al. 2014; Bonke et al. 2008); however, for longer oligomers, even this strategy often results in challenging purifications requiring careful preparative HPLC. Initially, this problem appeared simply to arise from incomplete conversion in the repetitive coupling cycles, involving these sterically demanding dimeric building blocks, leading to product mixtures apparently containing varying amounts of shorter oligomers with physicochemical properties very similar to the desired full-length oligomer. Nevertheless, frequent observations indicated that assembly of hybrids containing α-chiral β-peptoid residues led to more complex crude mixtures, even though the reacting sites may be considered equally congested. In addition, the recent attempts to obtain building blocks containing α-chiral benzyl side chains also carrying electron-donating substituents in the 4-position resulted in very poor yields (unpublished data). Thus, it was decided to examine whether these problems in fact originated from lack of stability of α-chiral benzyl-substituted amide functionalities in the presence of the strongly acidic conditions employed in the cleavage step upon assembly on solid phase. Besides examination of compounds **1** and **3** (displaying α-chiral and achiral β-peptoid residues, respectively), compound **6** was synthesized to also investigate the stability of α-chiral α-peptoid residues under the typical acidic conditions used for cleavage of Rink amide-linked peptidomimetics. Similarly, the antibacterial peptoid **7** (Jahnsen et al. 2012) was included in this part of the study as a representative of achiral peptoids.

The above-mentioned observations prompted us to optimize solid-phase oligomer assembly and cleavage from the resin by reducing the number of steps involved, while simultaneously facilitating purification by exploring the utility of tetrameric building blocks. Inspired by the use of trimeric β-peptoid building blocks (Shuey et al. 2006), prepared either by a solution-phase route or via solid-phase synthesis (SPS) (Hamper et al. 1998), we decided on a methodology combining solution-phase and solid-phase chemistry to obtain tetrameric building blocks. In addition, these measures were expected to afford less complex reaction mixtures

that might allow for more simple chromatographic purification, e.g., by reversed-phase vacuum liquid chromatography (RP-VLC).

Results and discussion

Even though several examples of SPS of α-chiral peptoids have been reported (Kirshenbaum et al. 1998; Wu et al. 2001; Gorske and Blackwell 2006; Fowler et al. 2009), there appears to be no reported studies on the stability of such peptidomimetics toward the strongly acidic conditions typically utilized in the final removal of side-chain protecting groups and release from acid-labile linkers. Hence, to determine whether acid-catalyzed degradation of full-length peptidomimetics contributes to the formation of byproducts present in crude mixtures obtained after cleavage from the resin, a simple stability study was performed. Here, a small amount of each selected peptidomimetic was subjected to prolonged exposure to tri-fluoroacetic acid (TFA), while samples continuously were analyzed by both MALDI-TOF and UHPLC at the following time points: 30 min, 1 h, 5 h, and 20 h. To enable the assessment of the influence of α-chirality, the test panel comprised compounds **1** and **6** as well as the achiral compounds **3** and **7**, which also allowed for an examination of whether α- or β-peptoid residues are equally sensitive to strongly acidic conditions (Fig. 2).

As evident from Fig. 2, nonchiral peptoid residues of both subtypes (e.g., in **3** and **7**) proved to be stable toward acid treatment even for prolonged periods, whereas both α-chiral subtypes (e.g., in **1** and **6**) were sensitive to extended exposure to strong acid. When comparing the stability of Nspe and βNspe residues, the latter were clearly more readily degraded, and to identify the nature of these byproducts formed, the distribution of molecular masses was analyzed in a time-dependent manner (Table 1).

Thus, it was found that all major degradation products arise from a simple acid-catalyzed debenzylation (Fig. 3), which relies on the formation of a secondary benzyl cation that is sufficiently stable to be readily formed under these conditions as opposed to the less stabilized primary benzyl cation involved in debenzylation of the corresponding achiral peptidomimetics. Thus, even short exposure to acid (e.g., for 30 min during cleavage) gives rise to a few more

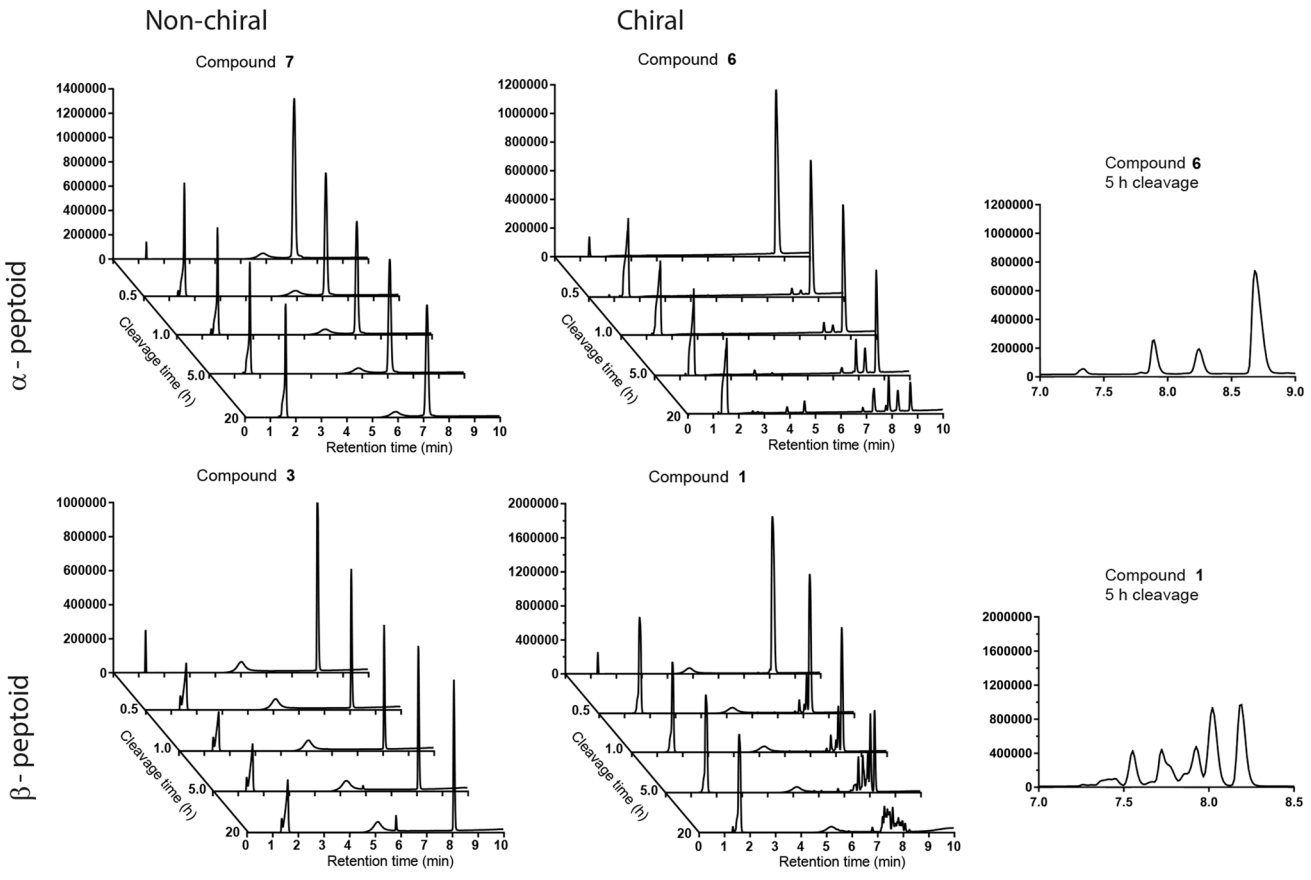

Fig. 2 Stability of α-peptide/α-peptoid hybrid **6** and α-peptoid **7** as well as that of α-peptide/β-peptoid hybrids **1** and **3** under acidic conditions (TFA)

Table 1 Time course of acid-catalyzed debenzylation of peptidomimetics with α-chiral peptoid residues

Time	Pam-(Lys-Nspe)$_3$ (**6**)[a]	Pam-(Lys-βNspe)$_6$ (**1**)[b]
0 h	$[M+H]^+$ (**s**)[c]	$[M+H]$ (**s**)
0.5 h	$[M+H]^+$ (**s**); $[M\text{-}Bn+H]^+$ (vw)	$[M+H]$ (**s**); $[M\text{-}Bn+H]^+$ (w)
1 h	$[M+H]^+$ (**s**); $[M\text{-}Bn+H]^+$ (w)	$[M+H]$ (**s**); $[M\text{-}Bn+H]^+$ (m); $[M\text{-}2Bn+H]^+$ (w)
5 h	$[M+H]^+$ (**s**); $[M\text{-}Bn+H]^+$ (m)	$[M+H]$ (**s**); $[M\text{-}Bn+H]^+$ (s); $[M\text{-}2Bn+H]^+$ (m); $[M\text{-}3Bn+H]^+$ (w)
20 h	$[M+H]^+$ (m);$[M\text{-}1Bn+H]^+$ (**s**); $[M\text{-}2Bn+H]^+$ (m); $[M\text{-}3Bn+H]^+$ (w)	$[M+H]$ (w); $[M\text{-}Bn+H]^+$ (m); $[M\text{-}2Bn+H]^+$ (**s**); $[M\text{-}3Bn+H]^+$ (m); $[M\text{-}4Bn+H]^+$ (w); $[M\text{-}5Bn+H]^+$ (vw); $[M\text{-}6Bn+H]^+$ (vw)

[a] *m/z* for: $[M\text{-}Bn+H]^+ = 1018$; $[M\text{-}2Bn+H]^+ = 914$; $[M\text{-}3Bn+H]^+ = 810$

[b] *m/z* for: $[M\text{-}Bn+H]^+ = 1971$; $[M\text{-}2Bn+H]^+ = 1867$; $[M\text{-}3Bn+H]^+ = 1763$; $[M\text{-}4Bn+H]^+ = 1659$; $[M\text{-}5Bn+H]^+ = 1556$; $[M\text{-}6Bn+H]^+ = 1451$

[c] The brackets indicate the intensity of peaks observed in the MALDI-TOF spectrum: *s* strong, *m* medium, *w* weak, *vw* very weak

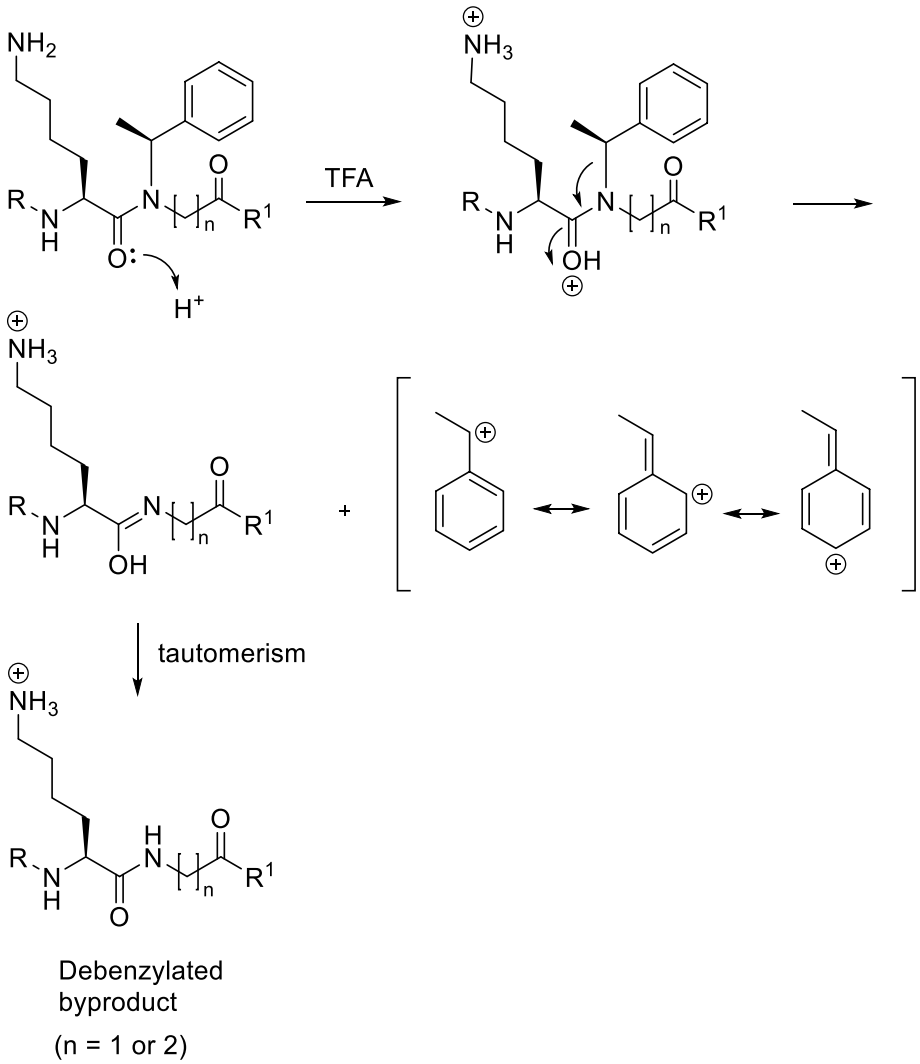

Fig. 3 Acid-catalyzed debenzylation of α-chiral peptoid residues

polar impurities for peptidomimetics displaying βNspe residues, while clearly detectable degradation of Nspe-containing peptidomimetics only occurs after more than 1 h. These findings have particular implications in the context of peptide/peptoid hybrids with a high content of Arg residues, since complete deprotection of the Pbf group, which is by far most commonly used protecting group for the guanidino functionalities, typically requires prolonged acidic cleavage for 1–12 h (Rothbard et al. 2002). Thus, the potential complication of achieving both complete

deprotection and avoiding degradation is important to consider, e.g., in case, synthesis of α-chiral analogs of well-known guanidinium-based cell-penetrating delivery vehicles (Stanzl et al. 2013; Schröder et al. 2008) is to be undertaken. Alternative routes, circumventing this issue, involve the use of bis(Boc)-protected guanidinylated building blocks (Bonke et al. 2008) that undergo fast cleavage, or of nosyl-protected building blocks that allow for a two-step on-resin conversion of amine functionalities into guanidinium side chains (Eggenberger et al. 2009).

Since the target immunomodulatory peptidomimetics **1**–**5** are headgroup-modified 12-meric oligomers, each consisting of a single dimeric repeating unit, it was envisaged that their tail moieties readily could be assembled on solid phase using either dimeric (Bonke et al. 2008) or tetrameric building blocks (i.e., **8**/**9** or **10**/**11**), thus avoiding difficult on-resin amide couplings involving the congested secondary amines of the β-peptoid residues. As dimeric building blocks **8** and **9** readily could be prepared on a multigram scale, an SPS protocol solely based on these was considered as a rapid and purification-free approach to obtain gram-scale amounts of appropriately protected tetramers **10** and **11** (Scheme 1).

To ensure the optimal conversion of the dimeric building block (i.e., **8** or **9**) in the attachment to the solid support, a threefold excess of the 2-chlorotrityl chloride (2-CTC) polystyrene (PS) resin was employed together with a large excess of diisopropylethylamine (DIPEA; 10 equiv). This procedure proved to be preferable over performing an initial neutralization step (typically with 10% DIPEA in dry CH_2Cl_2) to remove any residual acid present in the 2-CTC resin, as this, when carried out on a large batch of resin, led to partial hydrolysis of the linker. To further deplete the dimeric building block (**8**/**9**) from the filtrate obtained in the initial loading step, this was treated with another batch of 2-CTC resin (1.5 equiv), and then, the resulting resin portions were combined and capped. In fact, the resin constitutes a cheaper component than the dimeric building block that justifies its use in large excess. Moreover, this confers the benefits of downloading that ensures that only readily accessible sites are loaded, which, in turn, facilitates almost complete coupling of another congested dimeric building block.

Upon removal of the Fmoc-protecting group, the resin was subjected to coupling with a low excess (1.25 equivalents) of the appropriate dimeric building block to form the

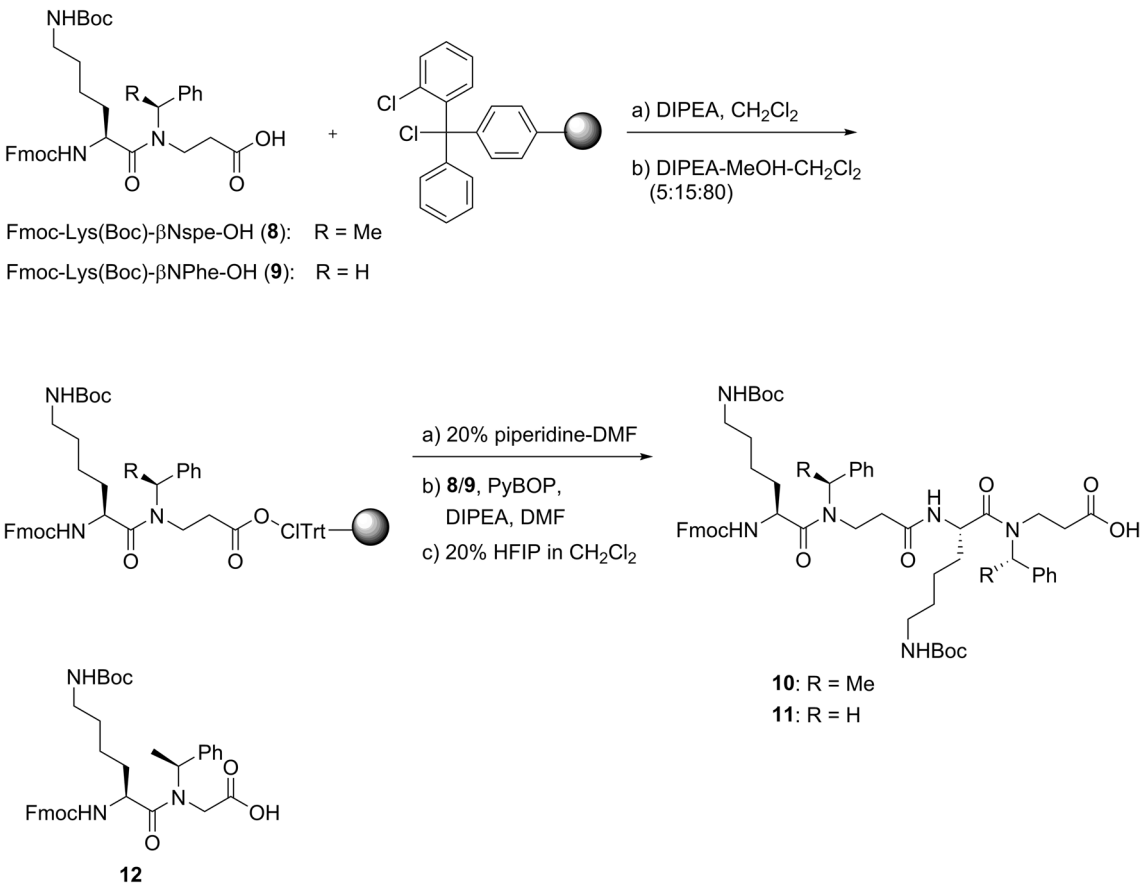

Scheme 1 Synthesis of tetrameric building blocks

desired Fmoc-protected resin-bound tetramer, which readily was cleaved off under mildly acidic conditions to afford the desired building blocks **10/11** in high overall yield (91% and 87%, respectively), and with sufficient purity (> 96.5% by UHPLC) to allow for direct use in oligomerization.

With both dimeric and tetrameric building blocks available in multigram amounts, their utility in both manual and automated MW-assisted SPS was investigated (Scheme 2 and Table 2). In manual synthesis (at room temperature), a threefold excess of resin was used during loading of **8/9** and **10/11** to ensure that the relatively large building blocks primarily were attached at readily accessible sites to ensure efficient chain elongation. To make a direct comparison in terms of atom efficiency, dimeric and tetrameric building blocks were used in 3- and 1.5-fold excess, respectively, while only 1 equivalent of both was used in the loading step. In manual SPS, a standard Rink amide PS resin and a relatively short coupling time of 2 h were employed to provide an overall cheap and rapid procedure. First, compound **1** was prepared by this manual protocol A (on a 0.2 mmol scale) using building block **8** or **10**. Due to the above finding that α-chiral β-peptoid residues only possess a limited stability under strongly acidic conditions, a short cleavage time (2 × 10 min) with immediate dilution of the drained product mixture with CH_2Cl_2-toluene prior to evaporation of TFA was employed. After purification by preparative HPLC, yields of 53% and 41% of compound **1** were obtained when using

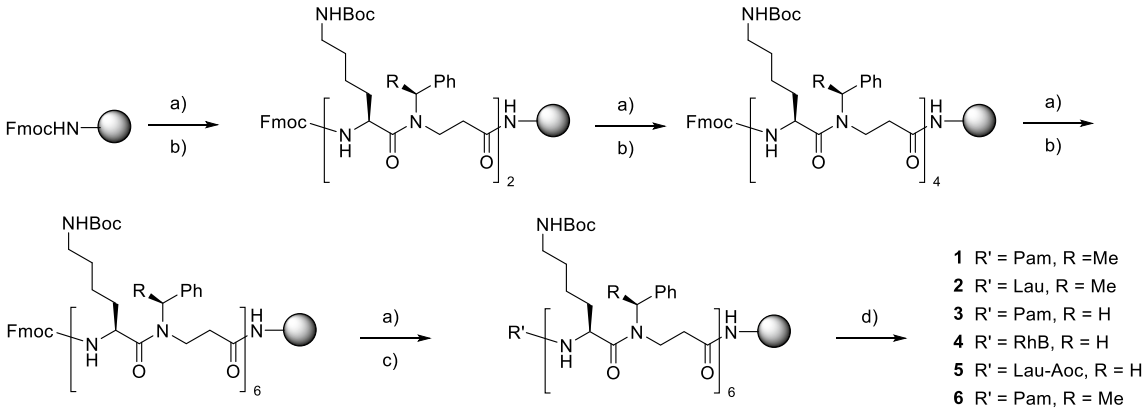

Scheme 2 Assembly of α-peptide/β-peptoid hybrids; shown with the use of tetrameric building blocks. Reagents and conditions: **a** 20% piperidine–DMF; **b 10/11**, PyBOP/DIPEA, HBTU/DIPEA, or DIC/Oxyma, DMF; **c** End-group modification: Lau-OSu/Pam-OSu, DIPEA, CH_2Cl_2; Fmoc-(*S*)-Aoc-OH or RhB, PyBOP, DIPEA, and DMF; **d** TFA-CH_2Cl_2 90:10. *DIC* diisopropylcarbodiimide, *HBTU* 2-(1*H*-benzotriazole-1-yl)-1,1,3,3-tetramethyluronium hexafluorophosphate, *Oxyma*: ethyl (hydroxyimino)cyanoacetate, *PyBOP* benzotriazole-1-yl-oxytripyrrolidinophosphonium hexafluorophosphate

Table 2 SPS of peptidomimetics **1**–**6** via different protocols

Entry	SPS protocol	Building block	Coupling conditions	Resin	Cmpd	Scale (mmol)	Amount (mg)	Yield (%)	Purity (%)
1	A	**8**	PyBOP 2 h	PS	**1**	0.2	291[a]	53	98.0
2	A	**10**	PyBOP 2 h	PS	**1**	0.2	228[a]	41	99.0
3	A	**10**	PyBOP 2 h	PS	**2**	0.5	439[b]	32	96.0
4	A	**11**	PyBOP 2 h	PS	**4**	0.1	66[a]	23	99.3
5	A	**11**	PyBOP 2 h	PS	**5**	0.5	665[b]	48	98.0
6	B	**8**	HBTU 10 min	CM	**1**	0.1	113[a]	40	99.5
7	B	**10**	HBTU 10 min	CM	**1**	0.1	79[a]	29	99.3
8	C	**9**	DIC/Oxyma 5 min	PS	**3**	0.1	104[a]	37	99.4
9	C	**11**	DIC/Oxyma 5 min	PS	**3**	0.1	43[a]	15	99.7
10	D	**9**	HBTU 10 min	PS	**3**	0.1	94[a]	34	99.1
11	C	**12**	DIC/Oxyma 5 min	PS	**6**	0.1	66[a]	45	99.8

CM ChemMatrix®, *PS* polystyrene

[a]Purified by preparative HPLC

[b]Purified by RP-VLC

dimer **8** (7 equiv. in total) and tetramer **10** (4 equiv. in total), respectively (Fig. 4; panels a and b).

The purity of the crude obtained for the tetramer-based synthesis of **1** proved to be comparable (albeit slightly improved with respect to closely eluting impurities) to that obtained in the corresponding dimer-based synthesis (Fig. 4, panels a and b). Even though the isolated yield was somewhat higher in the dimer-based protocol, it was considered appropriate to continue the exploration of tetramer-based SPS as it allowed for a reduced workload in terms of number of steps required for assembly. Thus, tetramer **10** was used to assemble compound **2** (displaying an N-terminal lauroyl moiety) in a larger scale (0.5 mmol) by protocol A, which was combined with an attempt to avoid the time-consuming preparative HPLC by using RP-VLC with a column packed with the standard C18 RP silica material (Merck RP-18 LiChroprep) instead. By this single-run procedure, 439 mg (yield: 32%) of compound **1** was isolated with a satisfactory purity (96%). Noticeably, conjugation to the fatty acid confers enhanced hydrophobicity to the impurities consisting of shorter oligomers, which facilitated elution by careful selection of a simple step gradient in the VLC. By contrast, compound **4**, displaying an N-terminal RhB moiety, proved more challenging to purify even by preparative HPLC due to its higher polarity, resulting in more closely eluting impurities. Thus, when **4** was prepared by manual SPS (0.1 mmol scale) using tetrameric building block **11,** a somewhat lowered yield of 23% was obtained; however, it should be recognized that, due to the presence of the RhB moiety, temporary separation of the open and closed forms obscured exact peak collection as previously observed for other RhB-labeled peptidomimetics (Birtalan et al. 2011). Finally, compound **5**, displaying two hydrophobic moieties (a fatty acid conjugated to a 2-aminooctanoic acid residue) leading to further improved peak separation, was also selected for synthesis in larger scale (0.5 mmol). Combined with purification by reverse-phase VLC, this allowed the isolation of 665 mg (48% yield; purity of 98.0%) after a single run.

Having established a robust protocol for manual solid-phase synthesis of this subtype of peptidomimetics (exemplified by **1**, **2**, **4,** and **5**), we decided to examine whether a tetrameric building block might be advantageous as compared to the corresponding dimeric building block, when employed in automated MW-assisted SPS followed by manual introduction of the fatty acid. The ChemMatrix® resin had previously proved superior to PS resins for assembly of difficult sequences due to its unique swelling properties (Garcia-Martin et al. 2006; de la Torre et al. 2007) and compatibility with MW heating (Bacsa et al. 2008). Hence, it was considered the first-choice solid phase in such a synthesis targeting compound **1** using HBTU as the coupling reagent. Somewhat surprisingly, the purities of the crudes

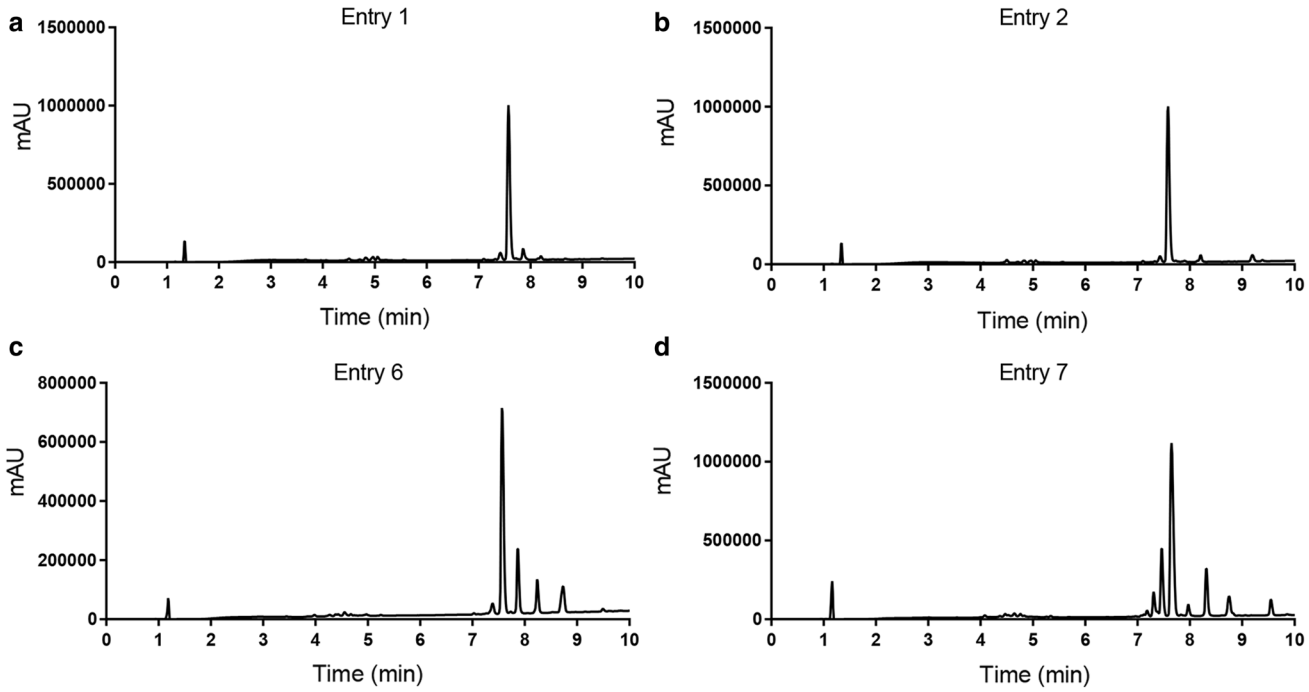

Fig. 4 Comparison of dimer- and tetramer-based SPS of compound **1**. In panels **a**–**d,** the crude mixtures obtained with different approaches are shown: **a** manual dimer-based SPS according to entry 1 in Table 2; **b** manual tetramer-based SPS according to entry 2 in Table 2; **c** MW-assisted dimer-based SPS according to entry 6 in Table 2; **d** MW-assisted tetramer-based SPS according to entry 7 in Table 2

obtained with both dimer **8** and tetramer **10** (Fig. 4, panels c and d) were less favorable than those obtained by manual synthesis using PyBOP as coupling reagent, despite the elevated coupling temperature (75 °C) and large excess of building blocks used (fivefold) versus the low excess (3- and 1.5-fold for **8** and **10**, respectively) sufficient in manual SPS at room temperature. This was also reflected in the lower isolated yields of **1** from MW-assisted syntheses (i.e., entries 6 and 7 in Table 2) as compared to manual syntheses (entries 1 and 2 in Table 2): 40% versus 53% (using dimer **8**) and 29% versus 41% (using tetramer **10**), respectively.

Next, compound **3** was prepared by MW-assisted SPS using both dimeric and tetrameric building blocks (i.e., **9** and **11**) followed by manual introduction of the N-terminal fatty acid moiety (Fig. 5; entries 8 and 9 in Table 2); in these cases, the coupling conditions DIC/Oxyma were employed on a PS resin, resulting in both crude purity and isolated yield of **3** (yield: 37%) comparable to those obtained for **1** (yield: 40%) when using the corresponding dimeric building blocks, while the use of tetramer **11** gave rise to a significantly lower isolated yield of **3** (15%). For comparison, a synthesis of **3** using HBTU on a PS resin (entry 10 in Table 2) was also included, and the similar result (yield: 34%) indicated that neither change in resin nor coupling conditions had a significant influence on the yield of the closely related peptidomimetics **1** and **3**. Finally, the short peptidomimetic **6** was obtained in 45% yield with the DIC/Oxyma conditions on a PS resin (entry 11 in Table 2).

Conclusion

In the present study, the stability properties of peptidomimetics displaying α- and β-peptoid residues resembling phenylalanine were examined. By performing a time-resolved analysis of the putative degradation under conditions corresponding to those used for cleavage, it proved possible to identify byproducts appearing in varying relative amounts in crude synthesis mixtures. While peptidomimetics displaying achiral peptoid residues were found to be stable for an extended period under the strongly acidic conditions, compounds containing α-chiral benzyl-based Nspe and βNspe residues underwent detectable debenzylation after 1 h. Interestingly, a βNspe-containing peptidomimetic was completely degraded after acid treatment overnight, thus excluding the combination of βNspe residues with the presence of multiple Pbf-protected arginine residues requiring prolonged cleavage time to ensure complete removal.

In addition, tetrameric building blocks were found to be applicable in efficient Fmoc-based SPS of larger amounts (100 mg to 1 g) of immunomodulatory lipidated α-peptide/β-peptoid hybrids by manual assembly on a standard PS resin. Importantly, the tetrameric building blocks could readily be prepared in gram scale by a purification-free solid-phase method giving high yields and sufficient purity for direct use in oligomerizations. In addition, selected crude mixtures proved amenable to purification by a single-run VLC, facilitated by the large retention differences observed between the desired product and the small impurities arising from tetramer deletions. In addition, the tetramer building blocks could be utilized in automated SPS with MW heating, albeit the purity of the crude products was not increased as compared to the use of dimeric building blocks in similar settings or to manual SPS. Thus, utility of these building blocks comprises both rapid assemblies of compound libraries for structure–activity studies as well as preparation of lead compounds in larger amounts.

Experimental

General

Starting materials were purchased from commercial suppliers and used without further purification: 2-Chlorotrityl chloride (2-CTC) polystyrene resin (loading: 1.70 mmol/g;

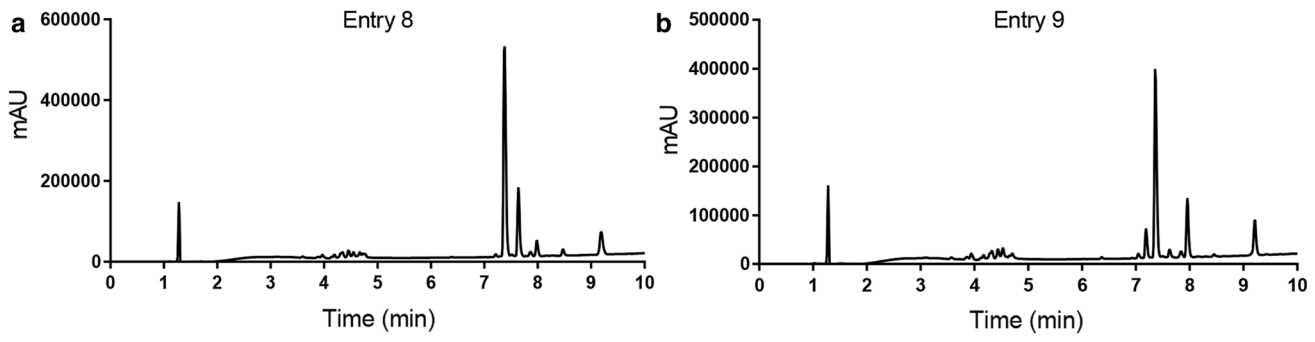

Fig. 5 Comparison of crudes for MW-assisted synthesis of compound **3** (using DIC). In panels **a**–**b,** the crude mixtures obtained with different approaches are shown: **a** dimer-based SPS according to entry 8 in Table 2; **b** tetramer-based SPS according to entry 9 in Table 2

Iris Biotech), Rink amide AM resin (loading: 0.71 mmol/g; Iris Biotech, Markredwitz, Germany), and ChemMatrix® Rink amide (loading: 0.53 mmol/g; Bio-Matrix Inc., Quebec, Canada), while Fmoc-Lys(Boc)-OH, Fmoc-(*S*)-Aoc-OH, di-*tert*-butyl dicarbonate (Boc_2O), HBTU, PyBOP, TBTU, DIC, OxymaPure®, DIPEA, piperidine, DMF, and NMP were from Iris Biotech. Pam-OSu, Lau-OSu, piperazine, *tert*-butyl acrylate, and Rhodamine B were from Sigma; (*S*)-α-methylbenzylamine from Merck; TFA from Alfa Aesar. Deionized water was filtered (0.22 µm) in-house by use of a Milli-Q plus system (Millipore, Billerica, MA). Vacuum liquid chromatography (VLC) was performed using silica gel 60H or 15–40 µm (Merck). Analytical UHPLC was performed on a Shimadzu Prominence UHPLC system using a Phenomenex Luna C18(2) HTS column (100 × 3.0 mm; particle size: 2.5 µm) eluted at a rate of 0.5 mL/min. Injection volumes were 5–10 µL of a ~ 1 mg/mL solution, and separations were performed at 40 °C. Eluents A (H_2O–MeCN–TFA 95:5:0.1) and B (MeCN–H_2O–TFA 95:5:0.1) were employed for linear gradient elution as indicated for each compound below. Preparative HPLC separations were performed on a Phenomenex Luna C18(2) column (250 × 21.2 mm; particle size: 5 µm or 250 × 30 mm; particle size: 5 µm) on a Shimadzu system consisting of a CBM-20A Prominence communication bus module, an LC-20AP Prominence pump, an SPD-M20A Prominence diode array detector, and an SIL-20A HT Prominence autosampler. The eluents A and B were employed with a flow rate of 20 mL/min or 40 mL/min; injection volumes were 300–900 µL. High-resolution mass spectrum of **6** was obtained on a Bruker MicroTOF-Q LC mass spectrometer equipped with an electrospray ionization source and a Quadrupole MS detector. The analysis were performed as ESI–MS (*m/z*): $[M + nH]^{n+}$.

Synthesis of dimeric building block 9

Fmoc-Lys(Boc)-OH (1.1 equiv, 21.9 g, 46.7 mmol), TBTU (1.5 equiv, 20.5 g, 63.7 mmol), and DIPEA (2.5 equiv, 185 mL, 106.2 mmol) were dissolved in CH_2Cl_2 (~ 10 mL/mmol). The mixture was stirred for 10 min, and then, the Michael adduct βNPhe-O*t*Bu (1 equiv, 10.0 g, 42.5 mL) (Bonke et al. 2008) was added in a minimum amount of CH_2Cl_2. The mixture was stirred at r.t. under N_2 for 16 h, after which the solvent was removed in vacuo. The residue was dissolved in EtOAc (1000 mL) and washed with 1 M HCl (3 × 500 mL), 0.1 M NaOH (2 × 500 mL), satd $NaHCO_3$ (500 mL), H_2O (2 × 500 mL), and brine (2 × 500 mL). Drying (Na_2SO_4), filtration and evaporation afforded a crude, which was purified on a VLC column (9.5 × 12 cm; heptane–EtOAc, 5:1–2:1) to give Fmoc-Lys(Boc)-βNPhe-O*t*Bu (Yield: 29.0 g; 91%).

The above intermediate ester was split in two equal portions, which separately were treated with TFA–CH_2Cl_2 (1:4, 150 mL) under stirring at r.t. for 2 h. The resulting mixtures were concentrated, and co-concentrated with CH_2Cl_2 and toluene several times. The two separate portions was dissolved in CH_2Cl_2 (200 mL), and then, Boc_2O (1.5 equiv, 7.0 g, 31.9 mmol) in CH_2Cl_2 (50 mL) and DIPEA (6 equiv, 22 mL, 128 mmol) were added. The mixture was stirred for 16 h at r.t., then diluted with EtOAc (1000 mL), and washed successively with 1 M HCl (2 × 500 mL), H_2O (8 × 100 mL), and brine (1 × 100 mL), dried (Na_2SO_4), filtered, and finally, the pH was adjusted to 7–8 before concentration. The residue was purified on a VLC column (12 × 12 cm; heptane-to-heptane–EtOAc 1:2 with 0.1% HOAc added) to give **9** (23.0 g; 87%); analyt. RP-HPLC: 98.6% at 220 nm ($t_R = 8.8$ min).

^{1}H NMR (600 MHz, CD_3OD): δ 7.79 (d, $J = 7.6$ Hz, 2H), 7.68–7.63 (m, 2H), 7.40–7.08 (m, 9H), 4.81* (d, $J = 17.0$ Hz, 1H), 4.71–4.54 (m, 3H), 4.40* (dd, $J = 7.0$, 10.6 Hz, 1H), 4.35–4.30 (m, 3H), 4.23 (t, $J = 6.8$ Hz, 1H), 4.18* (d, $J = 7.0$ Hz, 1H), 3.75–3.68* (m, 1H), 3.63–3.48 (m, 2H), 3.06–2.91 (m, 2H), 2.74–2.69* (m, 1H), 2.65–2.46 (m, 2H), 1.74–1.68* (m, 1H), 1.63–1.58 (m, 1H), 1.42* (s, 9H), 1.40 (s, 9H), 1.55–1.18 (m, 4H). *denotes additional signals from the minor rotamer; ^{13}C NMR (600 MHz, CD_3OD): δ 175.1, 174.9*, 174.7*, 174.4, 158.4, 158.3*, 145.2, 145.1, 142.5 (2C), 138.4, 138.1, 129.7, 128.7 (2C), 128.4*, 128.2, 128.1, 126.3*, 126.2, 120.9 (2C), 79.8, 67.9, 52.8, 52.6, 52.5*, 48.4, 44.2*, 44.1, 41.0*, 40.9, 34.2, 32.9, 30.6*, 30.5, 28.8 (3C), 24.0*, 23.9. * denotes additional signals from the minor rotamer; HRMS: calcd for $[M + Na]^+$ 652.2993, found 652.2992; $\Delta M = 0.1$ ppm.

Synthesis of tetrameric building blocks 10/11

In a glass funnel fitted with a glass filter (200 mL; Peptides International, Louisville, KY, USA), the 2-CTC resin (loading: 1.60 mmol/g; 5.0 g, 3 equiv) was briefly washed with dry CH_2Cl_2 (2 × 50 mL). To the drained resin, was then added a mixture of the corresponding dimeric building block (**8/9**; 1 equiv; 1.72 g/1.68 g, 2.67 mmol) and DIPEA (5 equiv, 2.32 mL, 13.3 mmol) in dry CH_2Cl_2 (25 mL), and loading was continued for 2 h under gentle shaking. The drained solution of dimeric building block was transferred to another batch of prewashed 2-CTC resin (2.5 g, 1.5 equiv), followed by gentle shaking for 2 h. The combined resin portions were capped with DIPEA–MeOH–CH_2Cl_2 (5:15:80, 2 × 10 min, 30 mL). Then, the resin was washed with CH_2Cl_2 (30 mL), Fmoc-deprotected with 20% piperidine in DMF (2 × 10 min), and washed with DMF, MeOH, and CH_2Cl_2 (each 3 × 5 min; 30 mL). A mixture of **8/9** (1.25 equiv, 2.13 g/2.10 g, 3.31 mmol), PyBOP (1.25 equiv, 1.72 g, 3.31 mmol), and DIPEA (2.5 equiv, 1.15 mL, 6.62 mmol) in DMF (25 mL) was allowed to react for 10 min, and was subsequently added to the resin, and then, the mixture was left under agitation for 16 h. Upon draining, the resin was

washed with DMF, MeOH, and CH_2Cl_2 (each 3 × 5 min; 30 mL). Cleavage of **10/11** from the resin was performed by treatment with 20% HFIP in CH_2Cl_2 (2 × 45 min, 20 mL). After concentration in vacuo, the residue was repeatedly dissolved in CH_2Cl_2 and evaporated again. Finally, residual solvent was removed on a freeze dryer to afford the tetrameric building blocks: Fmoc-[Lys(Boc)-βNspe]$_2$-OH (**10**; 2.70 g; 96% yield) and Fmoc-[Lys(Boc)-βNPhe]$_2$-OH (**11**; 2.36 g; 87% yield), respectively. For both the purity, HPLC was above 96.5%.

10: ^{1}H NMR (600 MHz, CD_3OD): δ 7.82 (d, J = 7.4 Hz, 2H), 7.72–7.68 (m, 2H), 7.45–7.21 (m, 14H), 5.45–5.26 (m, 1H), 5.05–4.99 (m, 1H), 4.90–4.80 (m, 1H), 4.64–4.55 (m, 1H), 4.45–4.34 (m, 2H), 4.29–4.19 (m, 1H), 3.52–3.34 (m, 3H), 3.24–3.14 (m, 1H), 3.12–2.97 (m, 4H), 2.72–2.35 (m, 3H), 2.26–2.10 (m, 1H), 1.79–1.30 (m, 36H); HRMS: calcd for $[M+H]^+$ 1069.5620, found 1069.5625; ΔM = 0.4 ppm.

11: ^{1}H NMR (600 MHz, CD_3OD): δ 7.79 (d, J = 7.2 Hz, 2H), 7.72–7.63 (m, 2H), 7.42–7.22 (m, 14H), 4.84–4.78 (m, 2H), 4.74–4.63 (m, 3H), 4.60–4.54 (m, 1H), 4.44–4.18 (m, 3H), 3.85–3.47 (m, 4H), 3.07–2.91 (m, 4H), 2.82–2.72 (m, 1H), 2.66–2.37 (m, 3H), 1.80–1.51 (m, 4H), 1.55–1.20 (m, 26H); HRMS: calcd for $[M+H]^+$ 1019.5488, found 1019.5490; ΔM = 0.1 ppm.

Synthesis of peptidomimetics

Protocol A (manual SPS of **1**, **2**, **4,** and **5**): the α-peptide/β-peptoid peptidomimetic was assembled on an Fmoc-Rink Amide polystyrene resin (loading: 0.7 mmol/g) in a Teflon reactor (10 mL; 0.2 mmol scale) or in a syringe (50 mL; 0.5 mmol scale) fitted with a polypropylene (PP) filter and a Teflon valve. The initial Fmoc deprotection was performed with 20% piperidine in DMF (each 5 mL or 20 mL, 2 × 10 min, with a 1-min DMF wash in between) followed by washing with DMF, MeOH, and CH_2Cl_2 (each 3 × 3 min with 5 mL or 20 mL). Loading of the first building block was performed using excess resin (3 equiv), while subsequent coupling of the appropriate building blocks (3 equiv of dimer **8/9** or 1.5 equiv of tetramer **10/11**) was performed with PyBOP (the same number of equiv as of building block used) and DIPEA (twofold excess as compared to PyBOP) in DMF (2 mL or 5 mL) for 2 h under shaking at room temperature. After loading, the resin was washed with DMF (3 × 3 min with 5 mL or 20 mL), capped with Ac_2O–DIPEA–NMP (1:2:3; 2 × 10 min; 5 mL or 20 mL), and then, washed with DMF, MeOH, and CH_2Cl_2 (each 3 × 3 min with 5 mL or 20 mL).

After the final Fmoc deprotection, the fatty acid moiety was introduced via coupling with the corresponding NHS ester: Lau-OSu or Pam-OSu (5 equiv) and DIPEA (5 equiv) in DMF (2 mL or 5 mL) during 16 h to ensure complete conversion. In compound **5**, the (*S*)-Aoc residue was introduced with Fmoc-(*S*)-Aoc-OH (5 equiv), PyBOP (5 equiv) and DIPEA (10 equiv) in DMF (5 mL) during 16 h to ensure complete conversion. Before cleavage, the resin was washed with DMF, MeOH, and CH_2Cl_2 (each 3 × 3 min with 5 mL or 20 mL). For compounds **1** and **2**, cleavage from resin was performed with TFA–CH_2Cl_2 (90:10; 2 × 10 min), while a prolonged cleavage time (2 × 45 min) was used for compounds **4** and **5**. All peptidomimetics were purified to homogeneity by preparative HPLC and/or vacuum liquid chromatography (VLC). The identity of the compounds was verified by MALDI-TOF, and the purity was determined by analytical HPLC (with detection at 220 nm). After lyophilisation, target compounds were stored at − 20 °C.

Protocol B The peptidomimetic was assembled (0.1 mmol scale) on a CEM Liberty Blue™ automated microwave synthesizer using Fmoc-based SPS on a H-Rink-Amide ChemMatrix® resin (loading: 0.53 mmol/g). Fmoc deprotection conditions: 20% piperidine in DMF (3 mL), initially 75 °C (MW, 100 W) for 30 s, and subsequently 75 °C (MW, 100 W) for 180 s. Coupling conditions: dimeric or tetrameric building block (5 equiv), HBTU (5 equiv), and DIPEA (10 equiv) at 75 °C (MW, 30 W) for 5 or 10 min. Upon assembly of the peptidomimetic, the resin was transferred to a Teflon vessel fitted with a PP filter using DMF. Upon draining, the resin was washed with DMF, MeOH, and CH_2Cl_2 (each 3 × 3 min with 3 mL) followed by palmitoylation and cleavage as in protocol A.

Protocol C The peptidomimetic was assembled (0.1 mmol scale) on a CEM Liberty Blue™ automated microwave synthesizer using Fmoc-based SPS on a polystyrene Fmoc-Rink Amide resin (loading: 0.70 mmol/g). Fmoc deprotection conditions: 10% piperazine in EtOH-NMP 1:9 (3 mL), initially 75 °C (MW, 100 W) for 30 s, and subsequently 75 °C (MW, 100 W) for 180 s. Coupling conditions: **9/11/12** (5 equiv), DIC (5 equiv, 1 mL), and Oxyma (10 equiv, 0.5 mL), at 75 °C (MW, 30 W) for 5 min. The palmitoylation step was performed as in protocols A and B. Then, the resin-bound peptidomimetics were subjected to cleavage from the linker with TFA–CH_2Cl_2 90:10 (3 mL, 2 × 45 min for compound **3**; 2 × 10 min for compound **6**, transferring the TFA solution into 30 mL toluene-CH_2Cl_2 1:1 that immediately was concentrated in vacuo).

Protocol D The peptidomimetic was assembled (0.1 mmol scale) as in protocol B on a CEM Liberty Blue™ automated microwave synthesizer using Fmoc-based SPS on a polystyrene Fmoc-Rink Amide resin (loading: 0.70 mmol/g). Fmoc deprotection conditions: 20% piperidine in DMF (3 mL), initially 75 °C (MW, 100 W) for 30 s, and subsequently 75 °C (MW, 100 W) for 180 s. Coupling conditions: dimeric or tetrameric building block (5 equiv), HBTU (5 equiv), and DIPEA (10 equiv) at 75 °C (MW, 30 W) for 10 min. The palmitoylation and cleavage steps were performed as in protocols A and B.

Compound **1** was prepared by protocols A and B: When using dimer **8** in protocol A followed by purification via preparative HPLC (gradient: 10% → 65% B in 20 min), this afforded compound **1** (291 mg; 53%) with a purity of 98.0% (analyt. UHPLC gradient: 10% → 80% B). When using tetramer **10** in protocol A, this afforded, similarly, compound **1** (228 mg; 41%) with a purity of 99.0%. When using dimer **8** in protocol B followed by purification via preparative HPLC (gradient: 10% → 65% B in 20 min), this afforded compound **1** (113 mg; 40%) with a purity of 99.5% (analyt. UHPLC gradient: 10% → 80% B in 10 min). When using tetramer **10** in protocol B followed by purification via preparative HPLC (gradient: 10% → 65% B in 20 min), this afforded compound **1** (79 mg; 29%) with a purity of 99.3% (analyt. UHPLC gradient: 10% → 80% B in 10 min).

Compound **2** was prepared by protocol A using tetramer **10** and purified on a VLC column (5 × 10 cm; Merck RP-18 LiChroprep 40–63 µm): initial conditioning with MeOH (500 mL), and then equilibration with 90:10 (500 mL) of HPLC solvents A and B. Fractions of 100–200 mL were collected when eluting with an increasing content of eluent B (A:B ratio): 90:10 (200 mL; fr. 1), 85:15 (200 mL; frs 2), 80:20, (400 mL; frs 3–4), 75:25, (400 mL; frs 5–6), 75.5:27.5 (2000 mL; frs 7–26); 70:30, (3000 mL; frs 27–48), 65:35, (200 mL; frs 49–50), 60:40, (200 mL; frs 50–51), and 55:45, (200 mL; frs 53–54). Fractions 30–50 were concentrated in vacuo and freeze-dried to give **2** as a white foam (439 mg; 32%) with a purity of 96.0% (analyt. UHPLC gradient: 10% → 80% B in 10 min).

Compound **3** was prepared by protocols C and D. When using dimer **9** in protocol C followed by purification via preparative HPLC (gradient: 10% → 60% B in 20 min), this afforded compound **3** (104 mg; 37%) with a purity of 99.4%. When using tetramer **11** in protocol C followed by purification via preparative HPLC (gradient: 10% → 60% B in 20 min), this afforded compound **3** (43 mg; 15%) with a purity of 99.7%. When using dimer **9** in protocol D followed by purification via preparative HPLC (gradient: 10% → 60% B in 20 min), this afforded compound **3** (94 mg; 34%) with a purity of 99.1%.

Compound **4** was prepared by protocol A. When using tetramer **11** followed by purification via preparative HPLC (gradient: 10% → 45% B in 20 min), this afforded compound **4** (66 mg; 23%) with a purity of 99.3%.

Compound **5** was prepared by protocol A and purified on a VLC column (5 × 10 cm; Merck RP-18 40–63 µm): initial conditioning with MeOH (500 mL), and then equilibration with 90:10 (500 mL) of HPLC solvents A and B. Fractions of 100–200 mL were collected when eluting with an increasing content of eluent B (A:B ratio) 90:10 (200 mL; fr. 1), 85:15 (200 mL; fr. 2), 80:20 (200 mL; fr. 3), 75:25 (400 mL; fr. 4), 72.5:27.5 (400 mL; frs 5–7), 70:30 (800 mL; frs 8–23), 67.5:32.5 (2400 mL; frs 24–39), 65:35 (1600 mL; frs 40–47), 60:40 (400 mL; frs 48–49), and 55:45 (800 mL; frs 50–53). Fractions 30–48 were concentrated in vacuo and freeze-dried to give **5** as a white foam (665 mg; 48%) with a purity of 98.0% (analyt. UHPLC gradient: 10% → 80% B in 10 min).

Compound **6** was prepared by protocol C. When using dimer Fmoc-Lys(Boc)-Nspe-OH (Jahnsen et al. 2014) followed by purification via preparative HPLC (gradient: 20% → 75% B in 20 min), this afforded compound **6** (66 mg; 45%) with a purity of 99.8% (analyt. UHPLC gradient: 10% → 80% B in 10 min).

Conditions for stability assessment

In the stability studies, each selected peptidomimetic (10 mg) was dissolved in TFA (500 µL), and then, samples (20 µL diluted with 500 µL milli-Q water) were analyzed by MALDI-TOF and UHPLC at the following time points: 30 min, 1 h, 5 h, and 20 h.

Acknowledgements We acknowledge Birgitte Simonsen for the purification of peptidomimetics. NMR equipment used in this work was purchased via Grant No. 10-085264 from The Danish Research Council for Independent Research|Nature and Universe.

Compliance with ethical standards

Conflict of interest The authors declare that they have no conflict of interest.

Informed consent All authors listed have contributed to conception, design, synthesis, gathering, analysis, or interpretation of data, and have contributed to the writing and intellectual content of the article. All authors gave informed consent to the submission of this manuscript.

References

Bacsa B, Horvati K, Bosze S, Andreae F, Kappe CO (2008) Solid-phase synthesis of difficult peptide sequences at elevated temperatures: a critical comparison of microwave and conventional heating technologies. J Org Chem 73:7532–7542. https://doi.org/10.1021/jo8013897

Bang JK, Nan YH, Lee EK, Shin SY (2010) A novel Trp-rich model antimicrobial peptoid with increased protease stability. Bull Korean Chem Soc 31:2509–2513. https://doi.org/10.5012/bkcs.2010.31.9.2509

Birtalan E, Rudat B, Kölmel DK, Fritz D, Vollrath SBL, Schepers U, Bräse S (2011) Investigating rhodamine B-labeled peptoids: scopes and limitations of its applications. Biopolymers 96:694–701. https://doi.org/10.1002/bip.21617

Bolt HL, Eggimann GA, Jahoda CAB, Zuckermann RN, Sharples GJ, Cobb SL (2017) Exploring the links between peptoid antibacterial activity and toxicity. MedChemComm 8:886–896. https://doi.org/10.1039/C6MD00648E

Bonke G, Vedel L, Witt M, Jaroszewski JW, Olsen CA, Franzyk H (2008) Dimeric building blocks for solid-phase synthesis of α-peptide–β-peptoid chimeras. Synthesis 2008(15):2381–2390. https://doi.org/10.1055/s-2008-1067171

Chongsiriwatana NP, Patch JA, Czyzewski AM, Dohm MT, Ivankin A, Gidalevitz D, Zuckermann RN, Barron AE (2008) Peptoids that mimic the structure, function, and mechanism of helical antimicrobial peptides. Proc Natl Acad Sci USA 105:2794–2799. https://doi.org/10.1073/pnas.0708254105)

de la Torre BG, Jakab A, Andreu D (2007) Polyethyleneglycol-based resins as solid supports for the synthesis of difficult or long peptides. Int J Pept Res Ther 13:265–270. https://doi.org/10.1007/s10989-006-9077-5

Eggenberger K, Birtalan E, Schröder T, Bräse S, Nick P (2009) Passage of Trojan peptoids into plant cells. ChemBioChem 10:2504–2512. https://doi.org/10.1002/cbic.200900331

Findlay B, Szelemej P, Zhanel GG, Schweizer F (2012) Guanidylation and tail effects in cationic antimicrobial lipopeptoids. PLoS One 7:e41141. https://doi.org/10.1371/journal.pone.0041141

Forsman H, Andréasson E, Karlsson J, Boulay F, Rabiet MJ, Dahlgren C (2012) Structural characterization and inhibitory profile of formyl peptide receptor 2 selective peptides descending from a PIP2-binding domain of gelsolin. J Immunol 189:629–637. https://doi.org/10.4049/jimmunol.1101616

Fowler SA, Blackwell HE (2009) Structure–function relationships in peptoids: recent advances toward deciphering the structural requirements for biological function. Org Biomol Chem 7:1508–1524. https://doi.org/10.1039/B817980H

Fowler SA, Luechapanichkul R, Blackwell HE (2009) Synthesis and characterization of nitroaromatic peptoids: fine tuning peptoid secondary structure through monomer position and functionality. J Org Chem 74:1440–1449. https://doi.org/10.1021/jo8023363

Garcia-Martin F, Quintanar-Audelo M, Garcia-Ramos Y, Cruz LJ, Gravel C, Furic R, Côte S, Tulla-Puche J, Albericio F (2006) ChemMatrix, a poly(ethylene glycol)-based support for the solid-phase synthesis of complex peptides. J Comb Chem 8:213–220. https://doi.org/10.1021/cc0600019

Goodson B, Ehrhardt A, Ng S, Nuss J, Johnson K, Giedlin M, Yamamoto R, Moos WH, Krebber A, Ladner M, Giacone MB, Vitt C, Winter J (1999) Characterization of novel antimicrobial peptoids. Antimicrob Agents Chemother 43:1429–1434. https://doi.org/10.1128/AAC.01080-10

Gorske BC, Blackwell HE (2006) Tuning peptoid secondary structure with pentafluoroaromatic functionality: a new design paradigm for the construction of discretely folded peptoid structures. J Am Chem Soc 128:14378–14387. https://doi.org/10.1021/ja065248o

Hamper BC, Kolodziej SA, Scatez AM, Smith RG, Cortez E (1998) Solid phase synthesis of β-peptoids: *N*-substituted β-aminopropionic acid oligomers. J Org Chem 63:708–718. https://doi.org/10.1021/jo971675w

Hansen PR, Munk JK (2013) Synthesis of antimicrobial peptoids. Methods Mol Biol 1047:151–159. https://doi.org/10.1007/978-1-62703-544-6_11

Hein-Kristensen L, Knapp KM, Franzyk H, Gram L (2011) Bacterial membrane activity of α-peptide/β-peptoid chimeras: influence of amino acid composition and chain length on the activity against different bacterial strains. BMC Microbiol 11:144. https://doi.org/10.1186/1471-2180-11-144

Holdfeldt A, Skovbakke SL, Winther M, Gabl M, Nielsen C, Perez-Gassol I, Larsen CJ, Wang JM, Karlsson A, Dahlgren C, Forsman H, Franzyk H (2016) The lipidated peptidomimetic Lau-((*S*)-Aoc)-(Lys-βNphe)$_6$-NH_2 is a novel formyl peptide receptor 2 agonist that activates both human and mouse neutrophil NADPH oxidase. J Biol Chem 291:19888–19899. https://doi.org/10.1074/jbc.M116.736850

Jahnsen RD, Frimodt-Møller N, Franzyk H (2012) Antimicrobial activity of peptidomimetics against multidrug-resistant *Escherichia coli*: a comparative study of different backbones. J Med Chem 55:7253–7261. https://doi.org/10.1021/jm300820a

Jahnsen RD, Haney EF, Franzyk H, Hancock REW (2013) Characterization of a proteolytically stable multifunctional host defense peptidomimetic. Chem Biol 20:1286–1295. https://doi.org/10.1016/j.chembiol.2013.09.007

Jahnsen RD, Sandberg-Schaal A, Vissing KJ, Nielsen HM, Frimodt-Møller N, Franzyk H (2014) Tailoring cytotoxicity of antimicrobial peptidomimetics with high activity against multidrug-resistant *Escherichia coli*. J Med Chem 57:2864–2873. https://doi.org/10.1021/jm401335p

Kim J-K, Lee S-A, Shin S, Lee J-Y, Jeong K-W, Nan YH, Park YS, Shin SY, Kim Y (2010) Structural flexibility and the positive charges are the key factors in bacterial cell selectivity and membrane penetration of peptoid-substituted analog of piscidin 1. Biochim Biophys Acta 1798:1913–1925. https://doi.org/10.1016/j.bbamem.2010.06.026

Kirshenbaum K, Barron AE, Goldsmith RA, Armand P, Bradley EK, Truong KTV, Dill KA, Cohen FE, Zuckermann RN (1998) Sequence-specific polypeptoids: a diverse family of heteropolymers with stable secondary structure. Proc Natl Acad Sci USA 95:4303–4308. https://doi.org/10.1073/pnas.95.8.4303

Kruijtzer JAW, Hofmeyer LJF, Heerma W, Versluis C, Liskamp RMJ (1998) Solid-phase syntheses of peptoids using Fmoc-protected N-substituted glycines: the synthesis of (retro) peptoids of Leu-enkephalin and substance P. Chem Eur J 4:1570–1580. https://doi.org/10.1002/(SICI)1521-3765(19980807)4:8%3c1570:AID-CHEM1570%3e3.0.CO;2-2

Lin H, Yan TT, Wang L, Guo FF, Ning GS, Xiong M (2016) Statistical design, structural analysis, and in vitro susceptibility assay of antimicrobial peptoids to combat bacterial infections. J Chemometr 30:369–376. https://doi.org/10.1002/cem.2801

Liu Y, Knapp KM, Yang L, Molin S, Franzyk H, Folkesson A (2013) High in vitro antimicrobial activity of β-peptoid-peptide hybrid oligomers against planktonic and biofilm cultures of *Staphylococcus epidermidis*. Int J Antimicrob Agents 41:20–27. https://doi.org/10.1016/j.ijantimicag.2012.09.014

Mojsoska B, Jenssen H (2015) Peptides and peptidomimetics for antimicrobial drug design. Pharmaceuticals 8:366–415. https://doi.org/10.3390/ph8030366

Mojsoska B, Zuckermann RN, Jenssen H (2015) Structure-activity relationship study of novel peptoids that mimic the structure of antimicrobial peptides. Antimicrob Agents Chemother 59:4112–4120. https://doi.org/10.1128/AAC.00237-15

Molchanova N, Hansen PR, Franzyk H (2017) Advances in development of antimicrobial peptidomimetics as potential drugs. Molecules 22:1430. https://doi.org/10.3390/molecules22091430

Norgren AS, Zhang S, Arvidsson PI (2006) Synthesis and circular dichroism spectroscopic investigations of oligomeric β-peptoids with α-chiral side chains. Org Lett 8:4533–4536. https://doi.org/10.1021/ol061717f

Olsen CA (2010) Peptoid-peptide hybrid backbone architectures. ChemBioChem 11:152–160. https://doi.org/10.1002/cbic.200900618

Olsen CA, Lambert M, Witt M, Franzyk H, Jaroszewski JW (2008) Solid-phase peptide synthesis and circular dichroism study of chiral β-peptoid homooligomers. Amino Acids 34:465–471. https://doi.org/10.1007/s00726-007-0546-8

Rothbard JB, Kreider E, Pattabiraman K, Pelkey ET, VanDeusen CL, Wright L, Wylie BL, Wender PA (2002) Arginine-rich molecular transporters for drugs: the role of backbone and side chain variations on cellular uptake. In: Langel Ü (ed) Cell-penetrating peptides: processes and applications. CRC Press LLC, Boca Raton, pp 142–160

Ryge TS, Frimodt-Møller N, Hansen PR (2008) Antimicrobial activities of twenty lysine-peptoid hybrids against clinically relevant bacteria and fungi. Chemotherapy 54:152–156. https://doi.org/10.1159/000119707

Schröder T, Niemeier N, Afonin S, Ulrich AS, Krug HF, Bräse S (2008) Peptoidic amino- and guanidinium-carrier systems: targeted drug delivery into the cell cytosol or the nucleus. J Med Chem 51:376–379. https://doi.org/10.1021/jm070603m

Shin SY (2014) Effect of double replacement of L-pro, D-pro, D-leu or Nleu in hydrophobic face of amphipathic α-helical model antimicrobial peptide on structure, cell selectivity and mechanism of action. Bull Korean Chem Soc 35:3267–3274. https://doi.org/10.5012/bkcs.2014.35.11.3267

Shuey SW, Delaney WJ, Shah MC, Scialdone MA (2006) Antimicrobial β-peptoids by a block synthesis approach. Bioorg Med Chem Lett 16:1245–1248. https://doi.org/10.1016/j.bmcl.2005.11.075

Simon RJ, Kania RS, Zuckermann RN, Huebner VD, Jewell DA, Banville S, Ng S, Wang L, Rosenberg S, Marlowe CK (1992) Peptoids: a modular approach to drug discovery. Proc Natl Acad Sci USA 89:9367–9371. https://doi.org/10.1073/pnas.89.20.9367

Skovbakke SL, Heegaard PMH, Larsen CJ, Franzyk H, Forsman H, Dahlgren C (2015a) The proteolytically stable peptidomimetic Pam-(Lys-βNSpe)$_6$-NH$_2$ selectively inhibits human neutrophil activation via formyl peptide receptor 2. Biochem Pharmacol 93:182–195. https://doi.org/10.1016/j.bcp.2014.11.004

Skovbakke SL, Larsen CJ, Heegaard PMH, Moesby L, Franzyk H (2015b) Lipidated α-peptide/*β*-peptoid hybrids with potent anti-inflammatory activity. J Med Chem 58:801–813. https://doi.org/10.1021/jm501341h

Skovbakke SL, Winther M, Gabl M, Holdfeldt A, Linden S, Wang JM, Dahlgren C, Franzyk H, Forsman H (2016) The peptidomimetic Lau-(Lys-βNSpe)6-NH2 antagonizes formyl peptide receptor 2 expressed in mouse neutrophils. Biochem Pharmacol 119:56–65. https://doi.org/10.1016/j.bcp.2016.09.004

Skovbakke SL, Holdfeldt A, Nielsen C, Hansen AM, Perez-Gassol I, Dahlgren C, Forsman H, Franzyk H (2017) Combining elements from two antagonists of formyl peptide receptor 2 generates more potent peptidomimetic antagonists. J Med Chem 60:6991–6997. https://doi.org/10.1021/acs.jmedchem.7b00489

Stanzl EG, Trantow BM, Vargas JR, Wender PA (2013) Fifteen years of cell-penetrating, guanidinium-rich molecular transporters: basic science, research tools, and clinical applications. Acc Chem Res 46:2944–2954. https://doi.org/10.1021/ar4000554

Wu CW, Sanborn TJ, Zuckermann RN, Barron AE (2001) Peptoid oligomers with α-chiral, aromatic side chains: effects of chain length on secondary structure. J Am Chem Soc 123:2958–2963. https://doi.org/10.1021/ja003153v

Zuckermann RN (2011) Peptoid origins. Pept Sci 96:545–555. https://doi.org/10.1002/bip.21573

Zuckermann RN, Kodadek T (2009) Peptoids as potential therapeutics. Curr Opin Mol Ther 11:299–307

Zuckermann RN, Kerr JM, Kent SBH, Moos WH (1992) Efficient method for the preparation of peptoids (oligo(N-substituted glycines)) by submonomer solid-phase synthesis. J Am Chem Soc 114:10646–10647. https://doi.org/10.1021/ja00052a076